

The quantum phase transitions of dimer chain driven by an imaginary ac field

C. S. Liu^{1,*}

¹*Hebei Key Laboratory of Microstructural Material Physics,
School of Science, Yanshan University, Qinhuangdao, 066004, China*

(Dated: September 9, 2020)

A topologically equivalent tight binding model is proposed to study the quantum phase transitions of dimer chain driven by an imaginary ac field. I demonstrate how the partner Hamiltonian is constructed by a similarity transformation to fulfil the \mathcal{PT} symmetry. The \mathcal{PT} symmetry of the partner model allows us to study the topological properties of the original non-Hermitian model as the Bloch bands of the Hermitian system. The quantum phase transitions are discussed in different frequency regime. The approach has the potential applications to investigate the topological states of matter driven by the complex external parameters.

I. INTRODUCTION

As pioneered by Yang and Lee in 1952, the quantum phase transitions (QPTs) can also be driven by the complex external parameters [1, 2]. It is believed that the introduction of the complex parameters at least gives a deep understanding QPTs [3]. The interest to study the issue is evoked recently by the realization of the static complex Zeeman field experimentally in non-Hermitian atomic systems by laser assisted spin-selective dissipations [4, 5]. The application of real ac fields has become a very promising tool to synthesize novel topological phase termed as Floquet topological engineering which otherwise would be impossible to achieve in the un-driven case [6–12]. A natural question that arises in this topic is what controllable characters of imaginary ac fields can bring to non-Hermitian systems although this kinds of field hasn't generated yet.

For the time-dependent Hamiltonian in the dipolar approximation, the relation between un-driven and driven system is given by the minimal coupling $\mathbf{k} \rightarrow \mathbf{k} + \mathbf{A}(t)$ where $\mathbf{A}(t)$ is the vector potential. One can obtain the time-dependent tight binding (TB) model with the time-dependent hopping $\tau(t)_{j,l} = \tau_{j,l} e^{i\mathbf{A}(t) \cdot (\mathbf{R}_j - \mathbf{R}_l)}$ in the inverse Fourier transform. However, for the case of imaginary ac field $\mathbf{A}(t) = i\mathbf{A}_0(t)$, $\tau(t)_{j,l} = \tau_{j,l} e^{-\mathbf{A}_0(t) \cdot (\mathbf{R}_j - \mathbf{R}_l)}$ and $\tau(t)_{j,l} \neq \tau(t)_{l,j}$ cause the imbalance hopping and non-Hermiticity of the Hamiltonian, which is contrast to the real ac field case $\tau(t)_{j,l} = \tau(t)_{l,j}$.

Generally, near the QPTs point, the external real parameters of the Hamiltonian drive the energy-levels crossing or avoided energy-level crossing between the ground state and the excited state. The global curvature in the parameter space can be captured by the geometric phase. Comparing the traditional analysis resorting to the order parameter and symmetry breaking within the Landau-Ginzburg paradigm, the geometric phases of the ground state provide a comprehensive reflection of the ground state characteristics in many-body systems. However, the non-Hermitian Hamiltonian exists the complex band structure and exhibits intriguing features with no counterpart in Hermitian cases [13–16] except for a non-Hermitian Hamiltonian having simultaneous parity-time (\mathcal{PT}) symmetry

[17, 18]. The imbalance hopping induces non-Hermitian skin effect which causes all eigenstates are localized exponentially to boundaries, regardless of topological edge states and bulk states [19–26]. In particular, the bulk-boundary correspondence is found recently to be breakdown completely for some non-Hermitian systems due to the skin effect [24, 27–32].

Concerning the non-Hermitian topological phases, the general Brillouin zone is used to understand the bulk-boundary correspondence of non-Hermitian system where a complex-valued wave vector is introduced to capture unique feature of non-Hermitian bands [19, 33–35]. The real part of the wave vector is from the periodicity of the system according to the Bloch theorem. The imaginary part of complex-valued wave vector is responsible for non-Hermitian skin effect. Experimentally, the non-Hermitian bulk-boundary correspondence has been demonstrated in discrete-time non-unitary quantum-walk dynamics of single photons [24] and in topoelectrical circuits [26].

Periodically driven non-Hermitian systems involve not only the non-Hermitian topological phases, but also Floquet topological phases. It has exhibit rich topological phases and non-Hermitian skin effect, without analogs in their static or Hermitian counterparts [31, 32, 36–39]. In particular, some of the studies focus on the periodic quenching a Hamiltonian from H_1 for the first half period to H_1 for the second one [31, 32, 37]. The key role played by periodic driving is changing symmetry and inducing an effective long-range hopping in lattice systems [40].

Controllable gain and loss of the available experimental setups make concrete realizations of non-Hermitian lattice model possible, such as a non-Hermitian version of the topological SSH model [41–44]. However, the non-Hermiticity induced by an imaginary ac field is not involved.

Motivated by the above considerations, I investigate the imaginary parameter driven QPTs by the analysis of an ac-driven dimer chain. I introduce a partner model without non-Hermitian skin effect that shares the same topological phase diagrams [45]. The partner of non-Hermitian Hamiltonian can be constructed by adjusting the imbalance hopping to fulfilling inverse or reflection symmetry. I demonstrate that partner Hamiltonian can be obtained by a similarity transformation and prove their topologically equivalent. In particular, the partner Hamiltonian have a \mathcal{PT} symmetry which allows to study the topological properties as the Bloch bands of the

* csliu@ysu.edu.cn

Hermitian system.

The merit of this method is that the bulk boundary correspondence is still effective without the introduction of the generalized bulk boundary correspondence and non-Bloch winding number. As shown below, the imaginary ac field drives the initial Bloch band splits into Floquet-Bloch bands. Interestingly, the ac-driven band inversion will lead to interesting topological states of matter which otherwise would be inaccessible in the real field case.

The remainder of this paper is organized as follows. In Sec. II, I present the 2D effective TB Hamiltonian of SSH model driven by an imaginary ac electric fields. I show how the amplitude of the vector potential controls the renormalization of the system parameters and leads to the non-Hermiticity of the effective Hamiltonian. In subsection III A, I present a partner model of the original model and illuminate that the original and modified models are related by a similarity transformation. Due to the topologically equivalence of the two model, I study the QPTs in low and intermediate frequency regime with the partner model in subsection III B and III C. Finally, I present a summary and discussion in Sec. IV.

II. MODEL

I consider the one-dimensional SSH model [46] driven by an imaginary ac electric fields. The imaginary ac electric field described by an imaginary vector potential $iA(t) = iA_0 \sin(\omega t)$ of frequency ω is applied in the chain direction. With the standard Peierls substitution $k \rightarrow k + A$, the Hamiltonian is given by $H(k, t) = \Psi_k^\dagger(t) h(k, t) \Psi_k(t)$ where $\Psi_k^\dagger(t) = [c_{k,A}^\dagger(t), c_{k,B}^\dagger(t)]$ and the non-Hermitian operator

$$h(k, t) = \begin{pmatrix} 0 & \tau + \tau' e^{A(t)} e^{-ik} \\ \tau + \tau' e^{-A(t)} e^{ik} & 0 \end{pmatrix}. \quad (1)$$

τ and τ' are the two hopping parameters of the dimer chain.

The model can be investigated by the Floquet-Bloch ansatz [47, 48]. The essence of this method is mapping the time-dependent Schrödinger equation to the eigen problem

$$\bar{h}(k, t) \Psi_k(t) = \Psi_k(t) \epsilon_k, \quad (2)$$

here

$$\bar{h}(k, t) = h(k, t) - i\partial_t = \begin{pmatrix} -i\partial_t & \tau + \tau' e^{A(t)} e^{-ik} \\ \tau + \tau' e^{-A(t)} e^{ik} & -i\partial_t \end{pmatrix}$$

is defined as the Floquet operator, and $\epsilon_k = \begin{pmatrix} \epsilon_{1,k} & 0 \\ 0 & \epsilon_{2,k} \end{pmatrix}$ is the quasienergy. The quasi-energies ϵ_k and the Floquet states $\Psi_k(0)$ can be obtained by diagonalizing the one-period propagator $U(T)$. The propagator $U(T)$ can be solved by integrating the following evolution equation numerically,

$$i \frac{\partial}{\partial t} U(t) = h(t) U(t).$$

in one period with the initial condition $U(0) = I_0$, here I_0 is the unit matrix.

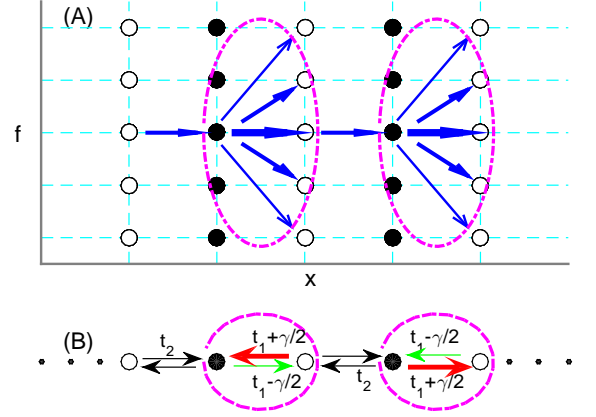


FIG. 1. (A) The effective 2D lattice of the periodically driven dimer chain. The additional f dimension is spanned by $\{n\}$ due to the time periodicity. The width of the arrows shows the hopping intensity qualitatively. (B) The partner model in the x direction. Adjusting the imbalance hopping between the adjacent unit cells (the magenta-dotted ellipse boxes) leads to the non-Hermitian skin effect disappearing in the x direction.

Alternatively, the driven dimer chain is mapped to time-independent 2D lattices. The quasienergy can be obtained by diagonalizing the effective Hamiltonian [48]. This method will be used in the following discussions and summarized briefly here. Using the Fourier transformation $\Psi_k(t) = \sum_n \Phi_{k,n} e^{in\omega t}$ and with the inner product $\langle\langle \cdot \cdot \rangle\rangle = \frac{1}{T} \int_0^T \langle \cdot \cdot \rangle dt$, the Floquet operator is transformed to

$$\bar{H}(k, k_f) = \sum_{m,n} \Phi_{k,m}^\dagger \bar{h}_{m,n} \Phi_{k,n}$$

$$\bar{h}_{m,n} = \begin{pmatrix} -n\omega\delta_{n,m} & \tau\delta_{n,m} + B_{m,n} \\ \tau\delta_{m,n} + B_{n,m} & -n\omega\delta_{n,m} \end{pmatrix} \quad (3)$$

where $\Phi_{k,\alpha}^\dagger = (c_{k,A,\alpha}^\dagger, c_{k,B,\alpha}^\dagger)$ with $\alpha = m, n$ and $B_{m,n} = \tau' e^{-ik} J_{m-n}(-iA_0)$, $B_{n,m} = \tau' e^{ik} J_{n-m}(iA_0)$. J_ν is the ν th Bessel function of the first kind. The diagonal term $-n\omega\delta_{n,m}$ of Eq. (3) is equivalent to an effective electric field ω in f direction and break the space inversion symmetry. Eq. (3) is an infinite matrix because n, m are integer. Shown in Fig. 1(A), the one-dimensional ac-driven model is exactly mapped to two dimensional TB problem in the composed Hilbert $\mathcal{S} = \mathcal{H} \otimes \mathcal{T}$, where \mathcal{H} is the ordinary Hilbert space and \mathcal{T} is the space of T-periodical function.

In the low frequency regime $\omega \ll \tau, \tau'$, the diagonal term $-n\omega\delta_{n,m}$ in Eq. (3) can be neglected. The Floquet operator is an effective TB model in the frequency space \mathcal{T} . The TB model can be transformed to the corresponding momentum k_f space:

$$\hat{h}(k, k_f) = \tau \begin{pmatrix} 0 & t_2 + t_- e^{-ika} \\ t_2 + t_+ e^{ika} & 0 \end{pmatrix}, \quad (4)$$

here

$$\begin{aligned} t_{1,\pm}(k_f) &= I_0 \pm \sum_{l=2n+1} 2(-1)^n I_l \sin lk_f \pm \sum_{l=2n} 2(-1)^n I_l \cos lk_f \\ &= t_1 \pm \frac{\gamma}{2}. \end{aligned} \quad (5)$$

Shown in Fig. 1(B), the TB model of the Floquet operator in Eq. (4) is dimer chain with the imbalance hopping $t_1 + \frac{\gamma}{2}$ in the left and $t_1 - \frac{\gamma}{2}$ right directions. I have used the relationship $J_{-v}(A_0) = (-1)^v J_v(A_0)$ and $J_v(iA_0) = i^v J_v(A_0)$, I_v is the v th modified Bessel function of the first kind [49]. In fact, the effective SSH model can also be written as

$$\hat{h}(k, k_f) = \tau \begin{pmatrix} 0 & t_+ + t_2 e^{-ika} \\ t_- + t_2 e^{ika} & 0 \end{pmatrix}. \quad (6)$$

The former is AB lattice and the latter is the BA lattice. They have the same phase transition point. The following discussions are focused on the equivalent BA lattice.

Out of the low frequency regime, we must diagonalize the one-period propagator $U(T)$ or the full Floquet matrix (3) to get the quasienergy due to the Floquet bands coupling. In the high frequency regime $\omega \gg \tau, \tau'$ however, the diagonal terms in Eq. (3) are important. The quasienergy bands have a large band gap ω and the matrix is approximately block diagonal. The topological phase transitions occur in the lowest Floquet band $m = n = 0$. In this case, the effective Hamiltonian in Eq. (3) is reduced to a the 2×2 hermitian matrix:

$$\tilde{h}_k = \tau \begin{pmatrix} 0 & I_0 + t_2 e^{-ik} \\ I_0 + t_2 e^{ik} & 0 \end{pmatrix}.$$

It is the SSH model and the topological phase transition occurs at $t_2 = \tau'/\tau = I_0$. This is different from the real ac field case where the topological phase transition occurs at $t_2 = J_0$ [48].

III. RESULTS

A. The partner model

The idea of constructing the partner Hamiltonian is from that the topological boundary states are protected by the symmetry of system and are immune to perturbations. It is reasonable to speculate that, for a class of non-Hermitian systems with non-Hermitian skin effect, there is a partner without non-Hermitian skin effect that has the same symmetry. As such, the topological invariants of the original models with non-Hermitian skin effect can be obtained from their partners, which share topological phase diagrams can be calculated in an easier way.

I construct the partner of the Floquet operator shown in Fig. 1(B). The reflection symmetry of the model is due to the change of the hopping terms $t_{1,\pm}$ alternately in the adjacent unit cell, and causes the skin effect to disappear [50]. For simplicity of the introduction, the diagonal term $-n\omega\delta_{n,m}$ in Eq. (3) is removed firstly and k_f is good quantum number. As shown below, the existence of the diagonal term

don't modify the conclusion. The partner Hamiltonian reads $\check{H}(k, k_f) = \Omega_k^\dagger \check{h} \Omega_k$ with

$$\check{h} = \begin{pmatrix} 0 & t_{1,+} & 0 & t_2 e^{-ik} \\ t_{1,-} & 0 & t_2 & 0 \\ 0 & t_2 & 0 & t_{1,-} \\ t_2 e^{ik} & 0 & t_{1,+} & 0 \end{pmatrix} \quad (7)$$

where $\Omega_k^\dagger(k_f) = (a_k^\dagger, b_k^\dagger, c_k^\dagger, d_k^\dagger)$ is the creation operation of the lattice (abcd) in unit cell of Fig 1. The partner Hamiltonian \check{h} has the \mathcal{PT} symmetry and follows the relation $[\mathcal{PT}, \check{h}] = 0$. \mathcal{P} and \mathcal{T} are defined as the space-reflection (parity) operator and the time-reversal operator, whose effects are given by $k \rightarrow -k, x \rightarrow -x$ and $k \rightarrow -k, x \rightarrow x, i \rightarrow -i$, respectively. The wave vectors k and k_f are real.

The partner model and original model are topologically equivalent. If we introduce a parameter θ in the model, i.e.

$$h(\theta) = \begin{pmatrix} 0 & t_1 + \frac{\gamma}{2} & 0 & t_2 e^{-ik} \\ t_1 - \frac{\gamma}{2} & 0 & t_2 & 0 \\ 0 & t_2 & 0 & t_1 - \frac{\gamma}{2} \cos \theta \\ t_2 e^{ik} & 0 & t_1 + \frac{\gamma}{2} \cos \theta & 0 \end{pmatrix}, \quad (8)$$

the original Hamiltonian \hat{h} of Eq. (5) can be continuously deformed into the partner Hamiltonian \check{h} of Eq. (7) when changing the parameter θ from π to 0. The Hamiltonian in Eq. (8) also has a chiral symmetry $\Sigma_z^{-1} h(\theta) \Sigma_z = -h(\theta)$ with $\Sigma_z = \sigma_0 \otimes \sigma_z$ and σ_0 and σ_z are unity matrix and the Pauli matrices respectively. The chiral symmetry ensures that the eigenvalues of Hamiltonian $h(\theta)$ appear in $(\varepsilon_j, -\varepsilon_j)$ pairs with $j = 1, 2$.

In the real-space, the original Hamiltonian \hat{h} and partner Hamiltonian \check{h} are related by a similarity transformation

$$\check{h} = S_0^{-1} \hat{h} S_0. \quad (9)$$

S_0 is a diagonal matrix whose diagonal elements are $\{1, r^2, r^2, r^2, \dots, r^{L/4}, r^{L/4+1}, r^{L/4+1}, r^{L/4+1}\}$ and $r = \sqrt{\frac{t_1 - \gamma/2}{t_1 + \gamma/2}}$ here L is the number of unit cell. The real-space eigen-equation $\hat{h}|\psi\rangle = E|\psi\rangle$ is equivalent to $\check{h}|\check{\psi}\rangle = E|\check{\psi}\rangle$ with $|\check{\psi}\rangle = S_0^{-1}|\psi\rangle$ where the eigenvalue E remains unchanged.

The diagonal matrix S_0 can be decomposed into the products of S_1 and S_2 ($S_0 = S_1 S_2$) where S_1 is a diagonal matrix whose diagonal elements are $\{1, r, r, r^2, r^2, \dots, r^{L-1}, r^{L-1}, r^L\}$ and S_2 is a diagonal matrix whose diagonal elements are $\{1, r, r, 1, \dots, 1, r, r, 1\}$. The modified Hamiltonian \check{h} can be constructed by two similarity transformations. With the similarity transformation as done in Eq.

$$\tilde{h} = S_1^{-1} \check{h} S_1, \quad (10)$$

\tilde{h} becomes the standard SSH model

$$\tilde{h} = (\tilde{t}_1 + t_2 \cos k) \sigma_x + t_2 \sin k \sigma_y$$

for $|t_1| > |\gamma/2|$, with intracell and intercell hopping $\tilde{t}_1 = \sqrt{(t_1 - \gamma/2)(t_1 + \gamma/2)}$ and $t_2 = \tau'$. This result has been obtained in Ref. [19]. Then doing the other similarity transformation $\check{h} = S_2^{-1} \tilde{h} S_2$, \check{h} becomes the partner Hamiltonian \check{h} in Eq. (7).

The corresponding eigenvalues $\hat{\varepsilon}$ of the original operator \hat{h} are complex and the corresponding eigenvalues $\check{\varepsilon}$ of the partner operator \check{h} are real. The relationship between $\hat{\varepsilon}$ and $\check{\varepsilon}$ can be understood as follow. The eigenvalues $\hat{\varepsilon}$ can be obtained by a unitary transformation, i.e. $\hat{\varepsilon} = \hat{U}_L^\dagger \hat{h} \hat{U}_R$, here $\hat{U}_L^\dagger \hat{U}_R = \hat{U}_R^\dagger \hat{U}_L = I_0$ and I_0 is the unity matrix. Due to the non-Hermiticity of operator \hat{h} , the unitary operator \hat{U}_L and \hat{U}_R must be differentiated. The corresponding eigenvalues $\check{\varepsilon}$ of the partner operator \check{h} can be obtained by the other unitary transformation $\check{\varepsilon} = \check{U}^\dagger \check{h} \check{U}$ and $\check{U}^\dagger \check{U} = \check{U} \check{U}^\dagger = I_0$. Due to the \mathcal{PT} symmetry of \check{h} , it is unnecessary to differentiate the left and right unity matrixs. From the relationship between the original and partner operators in Eq. (9), I can easy get the relationship of eigenvalue matrix between original and partner operators $\hat{\varepsilon} = U_L^\dagger \check{\varepsilon} U_R$. It is also a unitary transformation $U_L^\dagger U_R = U_R^\dagger U_L = I_0$ here the left and right unity matrixes must be distinguished with $U_L^\dagger = \check{U}_L^\dagger S_0 \check{U}$ and $U_R = \check{U}^\dagger S_0^{-1} \check{U}_R$.

It should point that this method is general effective to the model including the nearest-neighbor interaction only. When the next nearest-neighbor term t_3 exists in the model further, this method is general fail since it is difficult to guarantee the reflection symmetry of the t_2 and t_3 terms simultaneously under the similarity transformation.

When the diagonal term $-n\omega\delta_{n,m}$ in Eq. (3) is included in the model, we can also use this method to construct the partner model. The reason is that the similarity transformation of Eq. (10) is effectively applied to the x direction and the diagonal part $-n\omega\delta_{n,m}$ of matrix (3) remains unchanged since it is equivalence to electric field applying to the f direction. The \mathcal{PT} transformation also occurs in the x direction, the partner Hamiltonian also have the \mathcal{PT} symmetry and its eigenvalues are real. When changing the parameter θ from π to 0, the original Hamiltonian \bar{h} of Eq. (3) can be continuously deformed into the partner Hamiltonian and also remains $-n\omega\delta_{n,m}$ unchanged. So the partner is a topological equivalent to the original model.

B. Topological invariant and phase transition in low frequency limit

From Eq. (5), the external ac field modifies the effective hopping of the model which changes the QPTs. A_0 and k_f are adjustable parameters of the one dimensional problem. The Hamiltonian (4) and its partner (7) belongs to the BDI class, the winding number along the k direction is the topological invariant that differentiates the system from an ordinary insulator [48, 51]. To calculate the winding number of the partner Hamiltonian \check{h}_k in Eq. (7), the Hamiltonian \check{h}_k is transformed into block off-diagonal form

$$U\check{h}_kU^{-1} = \begin{pmatrix} 0 & 0 & t_1 + \frac{1}{2}\gamma & t_2 e^{ik} \\ 0 & 0 & t_2 & t_1 - \frac{1}{2}\gamma \\ t_1 - \frac{1}{2}\gamma & t_2 & 0 & 0 \\ t_2 e^{-ik} & t_1 + \frac{1}{2}\gamma & 0 & 0 \end{pmatrix} \quad (11)$$

with the unitary matrix

$$U = \begin{pmatrix} 0 & 0 & 0 & 1 \\ 0 & 1 & 0 & 0 \\ 0 & 0 & 1 & 0 \\ 1 & 0 & 0 & 0 \end{pmatrix}.$$

With the block off-diagonal Hamiltonian in Eq. (11), the winding number is defined by [52, 53]

$$\begin{aligned} \mathcal{W} &= - \oint \frac{dk}{2\pi i} \partial_k \left\{ \ln \left[\text{Det} \begin{pmatrix} \frac{1}{2}\gamma + t_1 & t_2 e^{ik} \\ t_2 & t_1 - \frac{1}{2}\gamma \end{pmatrix} \right] \right\} \\ &= - \oint \frac{dk}{2\pi i} \partial_k \left[\ln \left(t_1^2 - \frac{\gamma^2}{4} + t_2^2 e^{ik} \right) \right]. \end{aligned} \quad (12)$$

The winding vector is $t_1^2 - \frac{\gamma^2}{4} + t_2^2 e^{ik}$. We get the transition points are

$$t_1^2 = t_2^2 + \frac{\gamma^2}{4}, \quad (13)$$

namely, $\tilde{t}_1 = t_2$ which is just the results obtained in Ref. [19].

In the present example of the driven dimer chain, the topologically phase boundary is related with the equation (13). In the limit $A_0 \rightarrow 0$, $|\gamma/2| \rightarrow 0$ which results to $t_1 = \tau'/\tau = I(A_0) \rightarrow 1$. This is the phase transition point of bared SSH model. If we assume $A_0 \leq 1.5$, the contributions from $I_{l>6}(A_0)$ can be neglected. With a fixed A_0 , the parameter $|\gamma/2|$ in Eq. (5) can be taken in the range from the minimum $|\gamma_{\min}/2|$ to the maximum $|\gamma_{\max}/2|$ when changing k_f from 0 to 2π .

So the range of the parameter $\sqrt{t_1^2 - \gamma^2/4}$ is from $t_{1,\min} = \sqrt{I_0^2 - \gamma_{\max}^2/4}$ to $t_{1,\max} = \sqrt{I_0^2 - \gamma_{\min}^2/4}$. When $t_2 \geq t_{1,\max}$, the model is in the topological phase. While the case of $t_{1,\min} < |t_2| < t_{1,\max}$, there are some k_f with $|t_2| \geq \sqrt{t_1^2 - \gamma^2/4}$ and some k_f with $|t_2| < \sqrt{t_1^2 - \gamma^2/4}$. The former is corresponding to the topological phase and the latter is corresponding to the topological trivial phase. The model is in the topological phase, actually. When parameters $|t_2| < t_{1,\min}$ however, it is in the trivial case of SSH model. Therefore, the topological phase transition point is at $|t_2| = t_{1,\min}$. $|t_2| = t_{1,\min}$ as function of A_0 is plotted in Fig. 2 (blue solid line).

It is interesting to compare the phase boundary to the case driven by a real ac field. When the SSH model driven by a real ac field, the effective Hamiltonian $\hat{h}(k, k_f)$ is given by

$$\hat{h}(k, k_f) = \tau \begin{pmatrix} 0 & t_1 + t_2 e^{-ika} \\ t_1^* + t_2 e^{ika} & 0 \end{pmatrix},$$

here

$$\begin{aligned} t_1(k_f) &= J_0 + 2i \sum_{l=2n+1} J_l \sin lk_f + 2 \sum_{l=2n} J_l \cos lk_f \\ &= |t_1| e^{-i\theta}. \end{aligned} \quad (14)$$

Follow the analysis in the case of imaginary ac field, the topological phase transition point is at $t_2 = t_{1,\min}$. $t_2 = t_{1,\min}$ as function of A_0 is plotted in Fig. 2 (red dashed line).

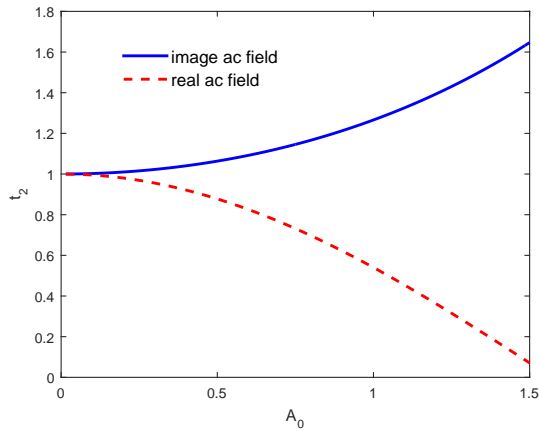


FIG. 2. The phase boundaries of the effective 2D lattice model driven by the imaginary ac field (blue solid line) and the real ac field (red dashed line). The upper part of the boundary is in topological phase and the lower part of the boundary is in insulator phase.

C. Beyond the low and high frequency limit

I study the partner model numerically to understand the topological phase beyond the low and high frequency limit. The eigenvalues of the equivalent model are real due to its \mathcal{PT} symmetry. Since the high level modified Bessel function compared with that of zero level are small enough to be neglected, I numerically diagonalize the partner of Eq. (3) without need a larger number of sidebands to reach convergence. In the present case $A_0 = 4$ and $I_7(A_0)/I_0(A_0) = 0.0037$, the matrix element $I_{m-n>7}$ can be neglected. Fig. 3 shows quasienergy spectrum vs A_0 for $n, m = 7$ sidebands.

When $\omega > 18$, the system is in the high frequency regime and the critical point $A_0 = 1.8079$ is almost fixed and meets $I_0(A_0) = t_2 = \tau'/\tau = 2$. When $A_0 > 1.8079$ in Fig. 3(a), the system exists the topologically protected states. With decreasing the frequency from the high frequency limit, the coupling between different Floquet bands cannot be neglected and induces the bands inversions near $A_0 = 4$ and $A_0 = 5.6$ in Fig. 3 (b). Bands inversions result to the opening and closing the band gap and change the topological properties of the model. The topological phase transition occur at the exact crossings between conduction and valence band in Fig. 3 (c).

IV. SUMMARY

In summary, with the Floquet-Bloch approach, we have mapped the dimer chain driven by an imaginary ac field to a

2D effective TB model to study the QPTs driven by an imaginary external parameter. To investigate the QPTs of the original non-Hermitian model, I construct a topologically equivalent model which fulfils the \mathcal{PT} symmetry. The merit of the method is the real energy spectra of the partner model allows to study the topological properties as the Bloch bands of the

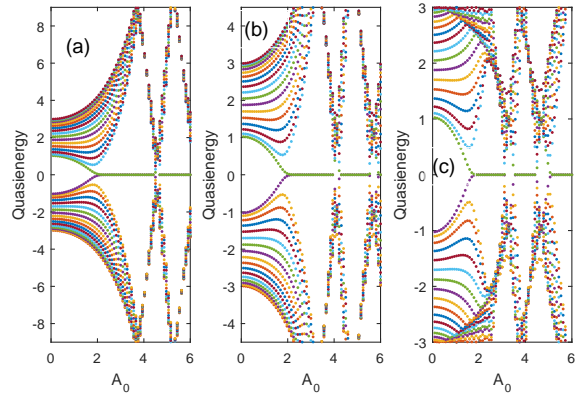


FIG. 3. Quasienergies ε of the equivalent tight binding model vs A_0 for different frequencies ω under open boundary conditions. (a) shows the quasi-energies near the high frequency limit $\omega = 16$, where the bands are not coupled. (b) the coupling between different Floquet bands leads the bands inversions and open a gap with the decreasing the frequency at $\omega = 12$. (c) shows the topological phase transition occurs at the exact crossings between conduction and valence band with $\omega = 6$.

Hermitian system without the introduction of the generalized Brillouin zone. The similarity transformation is given to illuminate the relationship between the partner Hamiltonian and the original Hamiltonian. I have obtained the phase boundary of driven dimer chain in different frequency regime. This method is expected useful to study the non-Hermitian systems with the non-Hermitian skin effect. The predicting novel topological states of matter which otherwise would be inaccessible in the real field case can be realized experimentally.

ACKNOWLEDGMENTS

This work was supported by Hebei Provincial Natural Science Foundation of China (Grant No. A2012203174, No. A2015203387) and National Natural Science Foundation of China (Grant No. 10974169, No. 11304270).

[1] C. N. Yang and T. D. Lee, “Statistical theory of equations of state and phase transitions. i. theory of condensation,” *Phys. Rev.* **87**, 404–409 (1952).

[2] T. D. Lee and C. N. Yang, “Statistical theory of equations of state and phase transitions. ii. lattice gas and ising model,” *Phys. Rev.* **87**, 410–419 (1952).

- [3] Victor Matveev and Robert Shrock, “On properties of the ising model for complex energy/temperature and magnetic field,” *Journal of Physics A: Mathematical and Theoretical* **41**, 135002 (2008).
- [4] Samantha Lapp, Jackson Ang’ong’a, Fangzhao Alex An, and Bryce Gadway, “Engineering tunable local loss in a synthetic lattice of momentum states,” *New Journal of Physics* **21**, 045006 (2019).
- [5] Jiaming Li, Andrew K. Harter, Ji Liu, Leonardo de Melo, Yogesh N. Joglekar, and Le Luo, “Observation of parity time symmetry breaking transitions in a dissipative floquet system of ultracold atoms,” *Nat. Commun.* **855**, 1 (2019).
- [6] V. M. Bastidas, C. Emary, B. Regler, and T. Brandes, “Nonequilibrium quantum phase transitions in the dicke model,” *Phys. Rev. Lett.* **108**, 043003 (2012).
- [7] Arijit Kundu and Babak Seradjeh, “Transport signatures of floquet majorana fermions in driven topological superconductors,” *Phys. Rev. Lett.* **111**, 136402 (2013).
- [8] Botao Wang, F. Nur Ünal, and André Eckardt, “Floquet engineering of optical solenoids and quantized charge pumping along tailored paths in two-dimensional chern insulators,” *Phys. Rev. Lett.* **120**, 243602 (2018).
- [9] M. Rodriguez-Vega and B. Seradjeh, “Universal fluctuations of floquet topological invariants at low frequencies,” *Phys. Rev. Lett.* **121**, 036402 (2018).
- [10] Haiping Hu, Biao Huang, Erhai Zhao, and W. Vincent Liu, “Dynamical singularities of floquet higher-order topological insulators,” *Phys. Rev. Lett.* **124**, 057001 (2020).
- [11] Jin-Yu Zou and Bang-Gui Liu, “Quantum floquet anomalous hall states and quantized ratchet effect in one-dimensional dimer chain driven by two ac electric fields,” *Phys. Rev. B* **95**, 205125 (2017).
- [12] Longwen Zhou and Jiangbin Gong, “Recipe for creating an arbitrary number of floquet chiral edge states,” *Phys. Rev. B* **97**, 245430 (2018).
- [13] Ingrid Rotter, “A non-hermitian hamilton operator and the physics of open quantum systems,” *Journal of Physics A: Mathematical and Theoretical* **42**, 153001 (2009).
- [14] Wenchao Hu, Hailong Wang, Perry Ping Shum, and Y. D. Chong, “Exceptional points in a non-hermitian topological pump,” *Phys. Rev. B* **95**, 184306 (2017).
- [15] C. Dembowski, B. Dietz, H.-D. Gräf, H. L. Harney, A. Heine, W. D. Heiss, and A. Richter, “Encircling an exceptional point,” *Phys. Rev. E* **69**, 056216 (2004).
- [16] Absar U. Hassan, Bo Zhen, Marin Soljačić, Mercedeh Khajavikhan, and Demetrios N. Christodoulides, “Dynamically encircling exceptional points: Exact evolution and polarization state conversion,” *Phys. Rev. Lett.* **118**, 093002 (2017).
- [17] Carl M. Bender and Stefan Boettcher, “Real spectra in non-hermitian hamiltonians having \mathcal{PT} symmetry,” *Phys. Rev. Lett.* **80**, 5243–5246 (1998).
- [18] C. Li, G. Zhang, X. Z. Zhang, and Z. Song, “Conventional quantum phase transition driven by a complex parameter in a non-hermitian \mathcal{PT} – symmetric ising model,” *Phys. Rev. A* **90**, 012103 (2014).
- [19] Shunyu Yao and Zhong Wang, “Edge states and topological invariants of non-hermitian systems,” *Phys. Rev. Lett.* **121**, 086803 (2018).
- [20] Shunyu Yao, Fei Song, and Zhong Wang, “Non-hermitian chern bands,” *Phys. Rev. Lett.* **121**, 136802 (2018).
- [21] Ching Hua Lee and Ronny Thomale, “Anatomy of skin modes and topology in non-hermitian systems,” *Phys. Rev. B* **99**, 201103 (2019).
- [22] Dan S. Borgnia, Alex Jura Kruchkov, and Robert-Jan Slager, “Non-hermitian boundary modes and topology,” *Phys. Rev. Lett.* **124**, 056802 (2020).
- [23] Stefano Longhi, “Probing non-hermitian skin effect and non-bloch phase transitions,” *Phys. Rev. Research* **1**, 023013 (2019).
- [24] Lei Xiao, Tianshu Deng, Kunkun Wang, Gaoyan Zhu, Zhong Wang, Wei Yi, and Peng Xue, “Non-Hermitian bulk-boundary correspondence in quantum dynamics,” *Nature Physics* **16**, 761–766 (2020).
- [25] Tobias Hofmann, Tobias Helbig, Frank Schindler, Nora Salgo, Marta Brzezińska, Martin Greiter, Tobias Kiessling, David Wolf, Achim Vollhardt, Anton Kabaši, Ching Hua Lee, Ante Bilušić, Ronny Thomale, and Titus Neupert, “Reciprocal skin effect and its realization in a topoelectrical circuit,” *Phys. Rev. Research* **2**, 023265 (2020).
- [26] T. Helbig, T. Hofmann, S. Imhof, M. Abdelghany, T. Kiessling, L. W. Molenkamp, C. H. Lee, A. Szameit, M. Greiter, and R. Thomale, “Generalized bulk-boundary correspondence in non-Hermitian topoelectrical circuits,” *Nature Physics* **16**, 747–750 (2020).
- [27] Tony E. Lee, “Anomalous edge state in a non-hermitian lattice,” *Phys. Rev. Lett.* **116**, 133903 (2016).
- [28] Ye Xiong, “Why does bulk boundary correspondence fail in some non-hermitian topological models,” *Journal of Physics Communications* **2**, 035043 (2018).
- [29] Flore K. Kunst, Elisabet Edvardsson, Jan Carl Budich, and Emil J. Bergholtz, “Biorthogonal bulk-boundary correspondence in non-hermitian systems,” *Phys. Rev. Lett.* **121**, 026808 (2018).
- [30] V. M. Martinez Alvarez, J. E. Barrios Vargas, M. Berdakin, and L. E. F. Foa Torres, “Topological states of non-hermitian systems,” *The European Physical Journal Special Topics* **227**, 1295–1308 (2018).
- [31] Hong Wu and Jun-Hong An, “Floquet topological phases of non-hermitian systems,” *Phys. Rev. B* **102**, 041119 (2020).
- [32] Xizheng Zhang and Jiangbin Gong, “Non-hermitian floquet topological phases: Exceptional points, coalescent edge modes, and the skin effect,” *Phys. Rev. B* **101**, 045415 (2020).
- [33] Kazuki Yokomizo and Shuichi Murakami, “Bloch Band Theory for Non-Hermitian Systems,” arXiv e-prints, arXiv:1902.10958 (2019).
- [34] Fei Song, Shunyu Yao, and Zhong Wang, “Non-Hermitian Topological Invariants in Real Space,” arXiv e-prints, arXiv:1905.02211 (2019).
- [35] Tian-Shu Deng and Wei Yi, “Non-bloch topological invariants in a non-hermitian domain wall system,” *Phys. Rev. B* **100**, 035102 (2019).
- [36] Bastian Höckendorf, Andreas Alvermann, and Holger Fehske, “Non-hermitian boundary state engineering in anomalous floquet topological insulators,” *Phys. Rev. Lett.* **123**, 190403 (2019).
- [37] Longwen Zhou and Jiangbin Gong, “Non-hermitian floquet topological phases with arbitrarily many real-quasienergy edge states,” *Phys. Rev. B* **98**, 205417 (2018).
- [38] Yang Cao, Yang Li, and Xiaosen Yang, “Non-Hermitian Bulk-Boundary Correspondence in Periodically Driven System,” arXiv e-prints, arXiv:2007.13499 (2020), arXiv:2007.13499 [cond-mat.mes-hall].
- [39] Longwen Zhou, “Non-hermitian floquet topological superconductors with multiple majorana edge modes,” *Phys. Rev. B* **101**, 014306 (2020).
- [40] Qing-Jun Tong, Jun-Hong An, Jiangbin Gong, Hong-Gang Luo, and C. H. Oh, “Generating many majorana modes via periodic driving: A superconductor model,” *Phys. Rev. B* **87**, 201109 (2013).

- [41] Julia M. Zeuner, Mikael C. Rechtsman, Yonatan Plotnik, Yaakov Lumer, Stefan Nolte, Mark S. Rudner, Mordechai Segev, and Alexander Szameit, “Observation of a topological transition in the bulk of a non-hermitian system,” *Phys. Rev. Lett.* **115**, 040402 (2015).
- [42] S. Weimann, M. Kremer, Y. Plotnik, Y. Lumer, S. Nolte, K. G. Makris, M. Segev, M. C. Rechtsman, and A. Szameit, “Topologically protected bound states in photonic parity-time-symmetric crystals,” *Nature Materials* **16**, 433 (2016).
- [43] Ananya Ghatak, Martin Brandenbourger, Jasper van Wezel, and Corentin Coullais, “Observation of non-Hermitian topology and its bulk-edge correspondence,” *arXiv e-prints*, arXiv:1907.11619 (2019), arXiv:1907.11619 [cond-mat.mes-hall].
- [44] Henning Schomerus, “Topologically protected midgap states in complex photonic lattices,” *Opt. Lett.* **38**, 1912–1914 (2013).
- [45] C S Liu J S Liu, Y Z Han, “A new way to construct topological invariants of non-hermitian systems with the non-hermitian skin effect,” *Chinese Physics B* **29**, 10302 (2020).
- [46] W. P. Su, J. R. Schrieffer, and A. J. Heeger, “Solitons in polyacetylene,” *Phys. Rev. Lett.* **42**, 1698–1701 (1979).
- [47] Grfonic M and Hänggi, *Phys. Rep.* **304**, 229 (1998).
- [48] A. Gómez-León and G. Platero, “Floquet-bloch theory and topology in periodically driven lattices,” *Phys. Rev. Lett.* **110**, 200403 (2013).
- [49] I.S. Gradshteyn and I.M. Ryzhik, *Table of Integrals, Series, and Products*, academic press ed., edited by Alan Jeffrey and Daniel Zwillinger (Translated from Russian by Scripta Technica, Inc., 2007).
- [50] Chun-Hui Liu, Hui Jiang, and Shu Chen, “Topological classification of non-hermitian systems with reflection symmetry,” *Phys. Rev. B* **99**, 125103 (2019).
- [51] Denis Bernard and André LeClair, “A classification of 2d random dirac fermions,” *Journal of Physics A: Mathematical and General* **35**, 2555–2567 (2002).
- [52] V. Gurarie, “Single-particle green’s functions and interacting topological insulators,” *Phys. Rev. B* **83**, 085426 (2011).
- [53] Zhong Wang and Shou-Cheng Zhang, “Topological invariants and ground-state wave functions of topological insulators on a torus,” *Phys. Rev. X* **4**, 011006 (2014).